Fracture 1977, Volume 1, ICF4, Waterloo, Canada, June 19 - 24, 1977

MICRO-MECHANISMS OF FRACTURE AND THE FRACTURE TOUGHNESS OF ENGINEERING ALLOYS

J. F. Knott*

ABSTRACT

The micro-mechanisms of cleavage and fibrous fractures in steels and aluminum alloys are reviewed and it is shown how local fracture parameters relate to macroscopic toughness values. For cleavage, emphasis is placed on the local tensile stress, σ_f, required to spread crack nuclei. The plastic work term is discussed, with respect to crack tip fracturing processes, and the relationship between σ_f and K_{IC} is developed. For fibrous processes, attention is paid to the crack opening displacement (C.O.D.) at initiation, δ_i, and it is shown that localized shear fractures in the matrix can reduce the values of δ_i that would be expected from void growth models. Finally, the occurrence of cleavage and fibrous fractures during fatigue crack propagation is described.

INTRODUCTION

The integrity of any engineering structure depends ultimately on the mechanical properties of the material of which it is made, and this paper is concerned with the extent to which it is possible to relate macroscopic measurements of fracture toughness in steels and aluminum alloys to the local micro-mechanisms of fracture. It proves convenient to divide the micro-mechanisms into two main types: *cracking processes*, which include transgranular and intergranular cleavage, and *rupture processes*, which include transgranular and intergranular fibrous fractures.

A material's plane-strain fracture toughness, K_{IC}, is conventionally measured as a critical value of the intensity, K_I, of the crack tip stress field in a thick, deeply-cracked testpiece subjected to mode I loading; see e.g., [1]. For the quasi-elastic fractures encountered when testing structural metals, local plastic flow around the tip of the precrack precedes fracture, but the value of K_I characterizes the crack-tip stress- and displacement-field, provided that the extent of plasticity is small, compared with specimen dimensions. Under such small scale yielding conditions, a critical value, K_{IC}, may be equated to a critical value of plastic-zone size or of crack-tip opening displacement (C.O.D.). For an infinite body in plane-strain, the plastic zone has the form of two lobes, whose maximum extent, R_{max}, lies at an angle of $\pm$ 70.5° to the line of crack extension, and whose minimum extent, R_{min}, is along this line [2]. In terms of K_I, R_{max} is given by:

$$R_{max} = 0.155 \left(\frac{K_I}{\sigma_Y} \right)^2 \qquad (1)$$

*Department of Metallurgy and Materials Science, University of Cambridge, Cambridge, United Kingdom.

and R_{min} is given by:

$$R_{min} = 0.04 \left(\frac{K_I}{\sigma_Y} \right)^2 \qquad (2)$$

The crack-tip opening displacement, δ, is given by:

$$\delta \simeq 0.5 \frac{K_I^2}{\sigma_Y E} \qquad (3)$$

where σ_Y is the uniaxial yield stress and E is Young's modulus. Critical values of K_I are then equivalent to critical values of R_{max}, R_{min}, or δ. In finite testpieces, the ratio of the in-plane stresses near the crack tip may modify the shapes of the plastic zones [3] and alter the numerical constants in equations (1) - (3), but the same general forms hold.

In terms of the micro-mechanisms of fracture, it is often physically appealing to interpret critical values of K_I (or of the equivalent values of potential energy release rate, G, or of contour integral, J) as a critical zone size or critical COD. For cracking processes, the plastic zone must increase in size until sufficient local stress has been generated to propagate a crack nucleus formed in some microstructural feature: for fibrous processes, the coalescence of voids formed around second-phase particles implies a critical crack tip displacement. The basic parameter represented by a K_{IC} toughness measurement may then differ for different fracture mechanisms. For pieces which fracture after amounts of plastic flow greater than that specified in the standard K_{IC} test procedure, (such that small-scale yielding approximations no longer hold) choice of a suitable toughness parameter, such as δ_c or J_{IC}, should be based on a clear understanding of the nature of the material's local fracture processes to enable effects of changes in geometry and stress-state to be properly explained.

CRACKING PROCESSES

Transgranular Cleavage

The transgranular cleavage fracture of low strength steel is a problem of major importance to the safe use of a wide variety of engineering structures. Plastic flow is necessary to produce crack nuclei [4] but, particularly in a structure, cracks may initiate and propagate at very low macroscopic strain, because the initial flow is usually localized to the region around a stress concentrator. Cleavage is favoured by low temperatures and high strain-rates, which increase the uniaxial yield stress, and by high triaxialities, which produce a high tensile stress for a given uniaxial yield stress. The metallurgical features which promote cleavage are those which increase the yield strength, whilst keeping the heat-treated microstructure unchanged: irradiation damage, pre-strain and strain-ageing. Refinement of grain-size increases the yield strength, but also improves a steel's resistance to cleavage fracture, conventionally because dislocation pile-ups are shorter, and hence less capable of initiating and assisting the propagation of cracks, in fine-grained material, e.g., [5, 6].

A detailed understanding of the role of microstructural features in determining the cleavage resistance of low strength steel derives from studies made on testpieces containing blunt notches.

The Critical Tensile Stress Criterion

Fracture may be considered to be *nucleated* when a critical value of *effective shear stress* is attained: this corresponding to a critically potent density of newly-created slip dislocations, which serves to fracture carbides, either by the stress induced at the end of a pile-up [7] or by plastically straining the matrix and producing sufficient stress transfer to crack the particle by a fibre-loading mechanism [8]. The nucleus *propagates* under a *tensile stress*, assisted by the local stress fields of the dislocations. For steels which are air-cooled (normalized) or furnace-cooled, the effective shear stress is independent of temperature, until such a low temperature is attained that plastic deformation occurs by twinning, rather than by slip [9]. In the Petch equation, written in terms of shear stress:

$$\tau_Y = \tau_i + k_Y^S \, d^{-1/2} \qquad (4)$$

where τ_Y is the shear yield stress, τ_i is the friction stress, and d is the grain diameter, the term k_Y^S is independent of temperature, at moderately low temperatures, unless the steel has been lightly quench-aged or strain-aged.

We consider the variation of plastic zone size at fracture in notched specimens at two low temperatures. At both temperatures, the effective shear stress component,

$$k_Y^S \, d^{-1/2},$$

is identical but the cracks nucleated at the lower temperature propagate when the plastic zone size is small, whereas those nucleated at the higher temperature do not. The reason for this is that fracture is *propagation-controlled* and depends on the level of the local *tensile* stress. At low temperatures, a crack nucleus can propagate when the plastic zone is small, because the yield stress is high (the friction stress, τ_i, increases markedly with decrease in temperature) and little elevation by constraint is then necessary to satisfy the local propagation condition. At higher temperature, the yield strength is smaller and so a higher hydrostatic component must be developed to achieve the critical propagation value for the tensile stress: this requires a larger plastic zone to produce the necessary constraint.

Values of the critical stress, σ_f, required to propagate nuclei in notched bars of mild steel have been obtained, employing stress analyses based on slip-line field theory [10, 11], (assuming rigid/perfectly plastic material) or finite element techniques [12, 13], (for elastic/plastic material). For slip-initiated cleavage fractures, σ_f is found to be only slightly temperature dependent. It is assumed that fracture begins to propagate below the notch root, at, or just behind, the plastic/elastic interface, where the tensile stress has a maximum value, (Figure 1).

Early micro-mechanical models of propagation-controlled, slip-initiated, cleavage fracture treated the propagation, either of a nucleus, formed by the interaction of slip dislocations [10, 14], or of a small crack formed in a grain boundary carbide [15]. The former model could not then explain effects of carbide width on fracture: the latter did not properly include the effects of stresses from local dislocation arrays on propagation. Currently, the most satisfactory model is one [7] which includes both features, giving, as an expression for the critical fracture stress, σ_f;

$$\left(\frac{Co}{d}\right)\sigma_f^2 + \tau_{eff}^2\left[\frac{1}{2} + \frac{2}{\pi}\left(\frac{Co}{d}\right)^{1/2}\frac{\tau_i}{\tau_{eff}}\right]^2 \geq \frac{4\,E\,\gamma_p}{\pi(1-\nu^2)d} \qquad (5)$$

where Co is the thickness of a grain boundary carbide,

$$\tau_{eff} = k_Y^S\, d^{-1/2}$$

is the effective shear stress, and γ_p is a surface energy or plastic work term. An equivalent expression has also been derived by Almond et al. [16]. The critical event is taken to be the propagation of a crack nucleus, formed in a grain boundary carbide, into the adjoining ferrite matrix. Figure 2 illustrates the process. Here, the microcrack formed in the (slanting) grain boundary carbide was just unable to propagate, whereas the microcrack formed in a thicker part of the carbide, and subjected to a marginally higher tensile stress, was able to propagate across the grain. Much more usually, particularly at low temperatures, arrest at the grain boundary does not occur and σ_f then corresponds to the carbide/ferrite propagation assumed in the model.

The critical tensile stress, σ_f, and associated parameters in equation (5) will be discussed in three contexts in the following sections. Firstly, experimental values of σ_f will be examined, to try to establish its microstructural significance; secondly, some comments on the meaning of γ_p will be made; finally, the use of σ_f to predict K_{IC} values will be demonstrated.

Microstructural Significance of σ_f

Figure 3 shows results, obtained by a number of authors, giving values of σ_f, in a variety of mild steels, as a function of the reciprocal square root of grain size. This parameter strictly has its basis only in a theory of propagation of a nucleus initiated by dislocation interaction [10, 14], but might generally be held to represent the effect of dislocation pile-up length. It is clear that σ_f does increase quite markedly with $d^{-1/2}$, although the scatter is large at high $d^{-1/2}$ values. A variation in the temperature at which σ_f was measured exists for most of the results, although the effect is small. Additionally, the results of Curry and Knott [17], which are at constant temperature (-120°C) follow the common trend. It is of interest to note that some points pertain to irradiated samples and that these do not differ significantly from those for non-irradiated specimens [18].

A problem arises if attempts are made to explain the $d^{-1/2}$ dependence using equation (5). Substituting

$$k_Y^S\, d^{-1/2}$$

for τ_{eff}, the equation becomes:

$$\left(\frac{Co}{d}\right)\sigma_f^2 + \left(k_Y^S\right)^2 d^{-1}\left[\frac{1}{2} + \frac{2}{\pi}(Co)^{1/2}\frac{\tau_i}{k_Y^S}\right]^2 \geq \frac{4\,E\,\gamma_p}{\pi(1-\nu^2)d} \qquad (6)$$

and the grain-size parameters cancel, leaving a relationship whose only microstructural parameter is carbide width, C_o. It has been suggested [19] that a possible reason for the apparent anomaly is that the development of microstructure by cooling from the austenitising temperature is such as to maintain the *ratio* of C_o/d constant, since both C_o and d depend

on similar diffusion phenomena. Curry has recently surveyed data on this point and has shown that there is a strong positive relationship between the two parameters although it is not quite linear. Using these (average) data and equation (5) he is able to construct a predicted failure line (shown schematically in Figure 4) whose precise position depends on γ_p and on the percentile of the carbide thickness distribution chosen to represent equally critical crack nuclei, i.e., the choice between for example, "10% of the carbides, having thicknesses of greater than 3μm" or "5%, having thicknesses greater than 4μm". The scatter in Figure 3 is then readily attributable to differences in carbon, or other alloy, content, of the steels, or to variations in heat-treatment. This point is reinforced by results obtained by Saunders [20] on a number of *low* (0.01) carbon, *equi-axed*, Fe-Cr and Fe-Ni alloys, which lie consistently just above the top of the scatter-band for the mild steels (Figure 4). The appropriate value of γ_p throughout is taken as 14 Jm^{-2}.

The strength of the dislocation contribution to the propagation criterion is a function of the ratio of Co to d [7]. For thin carbides, the crack nucleus does not extend far from the tip of the pile-up and so the dislocations have an important effect. For ratios in the range 0.1 - 0.15, however, as found in a number of structural mild steels, the dislocation stresses are of secondary importance, and the situation reduces virtually to that of the Griffith propagation of a crack of length equal to the grain boundary carbide thickness.

Recently, Curry has extended the model to cover low- and medium-carbon steels, heat-treated to produce spheroidal carbides. Again, the critical event appears to be the propagation of a nucleus, formed in the spheroidal carbide, into the ferrite matrix and a value of γ_p equal to 14 Jm^{-2} is appropriate. The dislocation contribution to propagation is ignored, because pile-ups as such do not occur. The dislocations tangle around carbides and tend to form a cell structure, whose dimensions depend on $X_o^{-1/2}$, where X_o is the inter-particle spacing, rather than on $d^{-1/2}$. The crack nucleus is taken to be *penny-shaped*, since it forms in a spheroidal particle, so that the expression for σ_f is given by:

$$\sigma_f = \left(\frac{\pi\,E\,\gamma_p}{2\,Co}\right)^{1/2} \qquad (7)$$

where Co is the carbide diameter. Taking Co at the 95th percentile of a given carbide distribution and spheroidal intra-granular carbides, the precise value of γ_p inferred from σ_f depends on an *a priori* assumption as to the size of the carbide from which the final crack propagated. This relates to the probability of finding a carbide of sufficient thickness in the region of high tensile stress ahead of the notch, which, in turn, depends on the shape of the carbide-size distribution function. Assuming that γ_p is constant, a given distribution of Co values will produce a distribution of σ_f values, derived from equations (5) or (7) multiplied by the probability of finding the appropriate carbide thickness in the appropriate region. The 95th percentile (γ_p = 14 Jm^{-2}) may be an overestimate, but results for the plate-like and spheroidal carbides are clearly consistent in that the same value of γ_p is obtained, assuming a mode I plane strain stress intensity factor in the former case and a "penny-shaped" factor in the latter. A reduction in the percentile figure chosen clearly brings a *pro rata* reduction in the inferred value of γ_p. Possible reasons for γ_p (up to 14 Jm^{-2}) being greater than the elastic work to fracture, $2\gamma_S$, (2 Jm^{-2}) will be presented in the following section.

In addition to the presence of carbide particles, high strength is imparted to steels by highly-dislocated martensitic substructures which, in low

carbon steels, divide the grains into "packets" or bundles of laths. A lath width is typically 0.2 - 2μm, and seems not to vary much with prior austenite grain size, although it does depend on the transformation temperature (low temperature martensite having narrow laths and higher temperature bainite having wider laths). The diameter of a packet (≈ lath length) may be an order of magnitude larger than the lath width and large misorientations occur across packet boundaries.

Work on the cleavage fracture of low carbon bainites and lath martensites has established that the microstructural feature controlling the resistance to crack propagation is the packet size [21, 22, 23]. Large deviations in the direction of propagation must occur at packet boundaries, (Figure 5), so that, if a crack begins in propagate in a single, favourably oriented packet, extra work must be done to allow it to propagate through an adjoining packet. Brozzo et al [22] consider that this is the critical event, provided that the packet size is sufficiently small. Their results are presented in Figure 4, together with a line representing a fracture criterion based on packet size:

$$\sigma_f = \left(\frac{4 E \gamma_p}{\pi (1-\nu^2) d_p} \right)^{1/2} \qquad (8)$$

where d_p is the packet diameter. The value of γ_p inferred from these results is 120 Jm^{-2}.

It is of interest to note that a single value for σ_f obtained by Green [24] for a bainitic A533B steel of 6μm packet size lies very close to the result of Brozzo et al. These results imply that there are two microstructural features which control cleavage resistance. In the mild steel ferrite/carbide type of microstructure, the carbides are of prime importance: in low carbon bainitic steels, packet size predominates. The importance of the dislocation substructure as compared with alloying elements in solid solution may be appreciated by contrasting the results of Brozzo et al with those obtained by Saunders on Fe-Ni and Fe-Cr alloys, having equiaxed grain structures (Figure 4). Values of σ_f in these alloys are superior to those in the mild steels, due to the low C content, but are inferior to those in the bainitic alloys, even though the total alloy content is similar. The relative importance of carbide distribution and packet size is treated also by Kotilainan and Törrönen [76].

Much progress has been made recently in the interpretation of σ_f in terms of critical events in a metallurgical microstructure, even though the mathematical relationships between σ_f and yielding and microstructural parameters are not yet fully developed. So far, events have been studied quantitatively in the more straightforward microstructures: ferrite plus grain-boundary carbide; ferrite plus spheroidal carbide; and, virtually, carbon-free lath martensites and bainites. Generally, regions of coarse microstructure are to be avoided, particularly if they are embedded in a harder matrix, because the higher yield stress of the matrix then increases the tensile stress level in the coarser, softer, region by constraint. The combination of high volume fraction of carbide together with a high transformation dislocation density, as found in most quenched and tempered forging steels, has yet to be examined to decide which propagation process is critical. It is of interest to note that an increased dislocation density, induced by prestrain, does produce higher values of σ_f in mild steel (from 1100 MPa to 1500 MPa for 25% strain at $d^{-1/2} = 7$), but simultaneously increases the matrix flow stress to a level such that the transition temperature also increases [25].

The Plastic Work Term

A value of γ_p which appears to give "reasonable" agreement between carbide size, grain size and σ_f, on the basis of equation (5) is 14 Jm^{-2}, although this figure could be lowered if a different view of the critical carbide size were taken. The value of $2\gamma_S$, the elastic work to fracture, is 2 Jm^{-2}. This discrepancy exists in other micro-mechanical models, but little consideration has been given to the reasons for it. The situation which must be examined in the present instance is one in which the critical event is the propagation of a crack nucleus from a grain-boundary carbide into the ferrite matrix.

For fracture to be propagation-controlled, it is essential that the value of γ increases, at some point, as the crack increases in length: if γ remains constant, fracture must be nucleation-controlled. A cementite carbide particle has higher modulus and, presumably, higher *true* surface energy than ferrite, so that "γ" would not be expected to increase, unless some of the applied potential energy were dissipated as plastic work before the nucleus started to propagate through the ferrite. An identical reason would be given to explain high values of γ_p for the propagation of sharp crack nuclei in a completely ferritic matrix. This "explanation", of "plastic work", does, however, beg the question of why it should be necessary to produce plasticity before a crack will propagate.

For a crack to propagate, the highly strained bond at its tip must fracture. It is usual to derive the force-displacement law for this crack-tip bond by simple differentiation of the curve of interatomic (or interionic) potential energy vs. displacement. The situation is modelled as a linear chair of two atoms, for which the energy exhibits a minimum at the rest position (the force is zero) and increases, to approach zero, as the atoms are separated to infinity. The maximum in the force-displacement curve occurs at the point of inflection at the energy-displacement curve, which is at a displacement of some 0.2 - 0.6 b_o, where b_o is the separation at the rest position, depending on the form of the bonding (metallic, ionic, covalent) [26]. Force may be converted to stress by dividing by appropriate lattice spacings, and if the resultant stress-displacement curve is approximated to half a sine-wave, the expression for the maximum stress becomes:

$$\sigma_{th} = \left(\frac{E \gamma_S}{b_o} \right)^{1/2} \qquad (9)$$

where $2\gamma_S$, the area under the curve, is taken as the energy per unit area required to separate the two atomic planes, or the elastic work to fracture, i.e., twice the energy per unit area of free surface, if it does not re-structure. The sine wave approximation may produce errors in detail, because it assumes a finite cut-off on the displacement axis, but in an iron lattice, screening potentials cause oscillations of the energy about zero at displacements of order b_o.

Treatments of crack-tip bond separation are generally based on the attainment of a critical stress, σ_{th}, whose magnitude is derived from improved forms of equation (9). For typical values of γ_S and b_o, σ_{th} is approximately E/10, although, for the specific case of the cleavage of iron across {100} planes, a figure of $E_{100}/3$ has been quoted, where E_{100} is measured in the [100] direction [27]. Materials generally have been divided into brittle or ductile types, depending on whether σ_{th} is attained in tension at the crack tip before sufficient shear stress is developed to

nucleate dislocations which can glide away from the tip on slip planes and produce blunting. A first approximation [27] gave the value of the necessary stress as $\tau_{th} \simeq 0.1\mu$ in iron, where μ is the shear modulus, but the energies involved in creating a dislocation loop which can expand under the influence of a shear stress, against lattice friction and image forces, have recently been re-examined [28]. The conclusions are consistent, on both approaches. Solids such as covalently bonded diamond, possessing high resistance to dislocation motion, are brittle; f.c.c. metals in which slip occurs easily, are ductile; b.c.c. iron is a borderline case.

For this borderline case, it is pertinent to examine the initial assumption, i.e., that the crack-tip bond "fractures" when the stress on that bond becomes equal to σ_{th}. This is clearly a necessary condition, and would also be sufficient for the model of a linear chain of two atoms: once at the position of maximum force, any increase in displacement would cause the atoms to separate catastrophically to infinity if the system were subjected to constant force (just as catastrophic failure occurs at the U.T.S. in a load-controlled testing machine).

The crack-tip environment does not, however, correspond to a load-control system. Once the displacement at σ_{th} has been exceeded, the crack-tip bond has negative stiffness, whilst every other bond "ahead" of, and "around" it has positive stiffness. The system is then much more akin to that of failure in a very "hard" (almost rigid) testing machine, where a critical displacement must be achieved. This displacement might be taken as $\sim b_o$ in the present case, and this would then represent the sufficient condition.

It is of interest to speculate on the events that might occur at crack-tip bond displacements between $0.5b_o$ (corresponding to the stress σ_{th} first being obtained) and b_o ("fracture"). Since, in iron, the balance between achieving a stress of σ_{th} in tension and a stress of τ_{th} is so fine, it is not inconceivable that τ_{th} might be attained at the sides of the crack tip during this further stretching of the bond. Dislocations could be created and glide a distance equal to a few Burgers vectors, sufficient to reduce somewhat the stiffness of the crack-tip environment, but not exceeding the saddle-point configuration, beyond which large-scale motion and blunting would occur. We might contemplate two dislocations (one on each side of the crack) each moving, say, three Burgers vectors, which may be equated roughly to three lattice spacings. If the stress acting on these were 0.1μ, the force per unit length on the dislocations would be approximately $0.1\mu b_o$ and so the total work done would be $0.6\mu b_o^2$ per unit length in the thickness direction. This extra work would have to be done to enable each successive crack-tip bond (spaced at b_o) to separate, so that the work per unit area associated with crack advance would be $0.6\mu b_o \simeq 0.24Eb_o$.

The value for $2\gamma_S$, 2 Jm^{-2}, corresponds to about $0.05Eb_o$ so that the increase in observed work to fracture produced by this type of mechanism would be of order five-fold. The difference between γ_p and $2\gamma_S$ found experimentally is about a factor of seven, so that the model has appeal, given the coarse approximations.

There are two further interesting points. Firstly, the extra work would have virtually no dependence on temperature, because the crack tip process are creation, and not thermally activated unpinning, of dislocations. The model therefore applies to an initially dislocation-free crystal, because if sources were present near the tip, dislocation generaltion from these would confuse the argument. Secondly, evidence of the dislocation generation would not necessarily be seen on stress-free fracture surfaces,

because, once the applied shear stress had been removed by advance of the crack tip, the image forces at the surface could be sufficient to pull back a dislocation which had not reached the saddle-point.

The atomic stress-displacement curve has also been approximated to a rectilinear form, with average stress, σ_1, up to a cut-off displacement, b_1, [26]. A region such as this existing ahead of a crack tip is equivalent to the Cottrell-Bilby-Swinden model for a yielded crack, and, for very low stresses, it is possible to write the size of the "end region" as

$$R = \frac{\pi E}{8(1-\nu^2)} \frac{b_1}{\sigma_1} \qquad (10)$$

Taking $\sigma_1 = 0.1$ E and $b_1 \simeq b_o$ as reasonable values, R is found to be about $4.5\ b_o$, so that the dislocation movement of $3b_o$ assumed earlier would be contained within this autonomous end region.

To summarize, it is suggested that, for iron, which is a borderline case with respect to brittle or ductile behaviour, it is necessary to consider displacement of the crack tip bond as the full fracture criterion, and that this may be associated with creation and very limited movement of crack tip dislocations which do plastic work of sufficient magnitude to explain the discrepancy between γ_p and $2\gamma_S$.

Relationship Between σ_f and Fracture Toughness

Even if the meaning of γ_p is not fully understood, it is clear, from Figure 3 or Figure 4, that it is possible experimentally to measure a value of σ_f which characterizes the critical value of tensile stress required to propagate a cleavage crack nucleus in a given microstructure. In a notched bar, the maximum tensile stress generated at a given temperature and strain-rate is determined by the size of the plastic zone. A similar situation holds, ahead of a sharp crack, with one important difference. For a blunt notch, the maximum value of the tensile stress increases as the plastic zone size increases, but, for a sharp crack, the absolute magnitude does not increase: the stress distribution extends over larger distances. For example, in Figure 6, the abscissa is the ratio of distance, X, to K^2/σ_Y^2; this means that, as K^2/σ_Y^2, or plastic zone size (equations (1, 2)) increases, so the absolute value of distance, X, increases, and a given stress level is produced at a greater distance from the crack tip.

Suppose that a particular value of σ_f has been measured in a notched bar, when a given ferrite/grain boundary carbide microstructure fractures. This is the stress required to propagate a nucleus formed in a sufficiently thick and favourably oriented carbide. It is reasonable to suppose that a pre-cracked specimen will fracture when a similar stress has been developed at the site of a suitable nucleus ahead of the tip of the pre-crack *(the critical distance)*. Ritchie et al [29] applied this model to explain the temperature variation of K_{IC} in mild steel. Taking an experimental value for σ_f, which was found not to vary with temperature over the range investigated, predictions of K_{IC} were made, assuming various fixed values of critical distance. Results are shown in Figure 7 and it is clear that the general trend is correct, although the authors pointed out that the excellent agreement obtained for a distance of two grain diameters was fortuitous.

The variation of critical distance with grain size has been further studied by Curry and Knott, [17] who showed that, in their mild steel, it was about four times greater than the grain diameter above about 50μm, but was apparently independent of grain size for finer grain sizes. A few confirmatory points have been obtained by Schulze [30]. The reason for this behaviour is that, at coarse grain size, the carbide distribution is such as to satisfy easily the propagation condition (equation (5)) whereas, in finer grain size it is not. More grains then have to be sampled to find a sufficiently thick carbide and the critical distance increases with respect to grain size. For example, taking γ_p as 14 Jm^{-2}, the experimental values for σ_f, when substituted into equation (5), give, for 12μm grain size, a critical nucleus size of just over 2μm and for 85μm grain size, a nucleus size of just over 6μm. It was observed experimentally that carbides of width 6μm occurred much more frequently in 85μm grain size than did those of width 2μm in 12μm grain size, so that a larger number of grains had to be sampled in the latter case, for the precracked specimen. (In fact, for the particular carbon content chosen, the 95th percentile thickness was about 0.1d, giving 8.5μm and 1.2μm respectively, compared with the "required" values of 6μm and 2μm).

The statistical treatment of plate-like grain boundary carbides is not easy, but Curry has recently extended the argument to spheroidal carbide microstructures. The fracture toughness, K_{IC}, and the critical distance can then be deduced quite accurately treating the 95th percentile as the critical carbide diameter, and taking γ_p = 14 Jm^{-2}, in terms of the probability of finding a sufficiently large carbide ahead of the crack.

The use of σ_f and critical distance to predict K_{IC} has great value in the prediction of the failure criterion for large, thick, engineering components provided that stress analysis is sufficiently good to give local tensile stress levels and to quantify increases or decreases in constraint as plastic zones develop. Some promise is given by results on A533B obtained by Parks [31] and by Green [24]: the latter finds that the critical distance is about five "packet" diameters, but emphasizes that *transitions* to ductile behaviour can occur at unrealistically low temperatures, because of stress relaxation by gross plastic flow in small testpieces. The use of σ_f is of particular interest with respect to surveillance specimens for neutron irradiation: if σ_f itself is not altered by irradiation, predictions of toughness changes can be made from small specimen results.

Intergranular Cleavage

One form of brittle fracture that occurs, particularly in higher strength forging steels, involves the fast propagation of cracks along prior austenite grain boundaries, which have been weakened by the accumulation of minor impurity elements, especially those from groups IV, V and VI of the Periodic Table [32]. An example is shown in Figure 8, which is of an as-quenched steel, containing rather high Mn and P contents. Grain-boundary embrittlement will be treated elsewhere; for the present, several possibilities may be recognized:

a) as-quenched embrittlement (as Figure 8) caused by segregation in austenite. In some cases this may be removed by very high temperature heat-treatment.

b) lack of as-quenched embrittlement, but development of intergranular fracture at tempering temperatures around 350°C (500°F) - see paper by Tait and Knott [33]. Such embrittlement may be caused by rejection of an impurity element (presumably P) by growing carbides [34, 35]. At higher temperatures, the element may diffuse away from the boundary. This

mechanism is one possible reason for the lowering of toughness in the critical tempering range, presumably at a point where grain boundary carbides (crack nuclei) are quite large, but the matrix yield strength is also high, and the segregated boundary provides a low-energy path. The addition of Si to steels, such as 300M undercarriage forging material, retards carbide growth and shifts the toughness minimum to higher tempering temperatures. A minimum could also occur in the absence of segregation, due to a critical balance between matrix strength and carbide size; alternatively, inter-lath retained austenite may transform to cementite and produce brittle particles [36]. Study of the fracture path is obviously an important factor in deciding between these mechanisms; see [77].

c) reversible temper embrittlement, which is caused by carbide rejection or equilibrium segregation of impurity elements to prior austenite grain boundaries during cooling after tempering. Interactive effects, such as those between Ni and Sb, may enhance the amount of segregation that occurs.

In each case, a segregated boundary must be held to represent a path along which the work to fracture is low, compared with that of transgranular cleavage. In case (c) particularly, it is possible to develop identical microstructures in terms of prior austenite grain size, recrystallized ferrite grain size and tempered carbide distribution, and to obtain a transition from cleavage to intergranular fracture, with consequent decrease in toughness, simply by altering the amount of segregation by varying the cooling rate after tempering.

Only a few measurements of σ_f in unsegregated and segregated alloy steel have been made [37], and these have not been related quantitatively to the microstructure. For En30A (0.4C, 4.25Ni, 1.5Cr), the value for an unembrittled steel at 77K was approximately 2200 MPa: for the same steel embrittled for 24h at 500°C, σ_f dropped to approximately 1250 MPa. The former figure is similar to that for A533B (Figure 4) and it is plausible that the recrystallised ferrite grain size in the En30A was similar to the packet size in A533B. For neither embrittled nor non-embrittled steel is it really possible to relate σ_f to γ_p through equation (5), because the high volume fraction of tempered carbides prevents the formation of pile-ups, inherent to the model. Assuming that the crack nuclei are the same in both cases and treating them as Griffith cracks, the approximate factor of two reduction in σ_f implies a factor of four reduction in γ_p. A similarly embrittled steel with slightly coarser carbides showed a further reduction in σ_f, to about 1150 MPa.

The reason for the inferred reduction in γ_p is by no means clear. The final value is still greater than the elastic work to fracture for pure iron. The amount of segregated species on a boundary may approach the monolayer level, but intergranular fracture can be obtained with much lower coverage than this. In terms of the previous discussion of the meaning of γ_p, it is unlikely that the presence of segregant will affect the crack-tip dislocation generation process as such, but there might be a strong influence on the shape of the interaction energy curve, i.e., on the cohesive strength of iron-iron pairs across a boundary. Iron relies for its bonding mainly on 3d electrons, a proportion of which are unpaired. It is, perhaps, significant that those elements which cause embrittlement (from groups IV, V and VI) possess large numbers of electrons, in the outer shell, which may be able to alter significantly the energy levels in the 3d band and effectively weaken the bonding. The details of such a process are not known, but it is likely that rather less crack tip dislocation movement would then be necessary to allow the crack tip bond to

fracture.

Critical distance values of one or two grain diameters have been derived for intergranular fractures [37], but the interpretation of such figures, even on a statistical basis, is, as yet, lacking. Generally, such fracture processes need to be studied in much more detail, with the aim particularly of assessing the effect that a given impurity element content has on toughness. Recycling trends are leading to a gradual increase in impurity levels in steels and it is of prime importance to be able to predict whether such higher levels will have significant deleterious consequences with respect to the integrity of engineering components.

RUPTURE PROCESSES

Transgranular Fibrous Fracture

At moderately high temperatures, for steels, and generally, for aluminum alloys, cracks do not propagate by a brittle cleavage mechanism, but by the linkage of voids, formed around second-phase particles. If particles are bonded strongly to the matrix, it is necessary to nucleate voids by subjecting the particles to high stresses from dislocations tangling around them. Nucleation then depends on a critical dislocation density or shear strain. For most non-metallic inclusions in steel, however, the bonding is so weak that voids form at almost zero strain. In some aluminum alloys, intermetallic particles, although reasonably well bonded, are inherently weak, and may crack, to form void nuclei. It is not clear whether such a process depends simply on the tensile stress level or whether particles are fibre-loaded by matrix plastic strain.

Once initiated, voids grow under the influence of an applied tensile stress but a lateral stress seems also to be necessary if the voids are to grow sideways as well as lengthways. Under such conditions, the fracture ductility may be calculated as a function of the volume fraction of voids, assuming either that they grow until they touch [38] or that they approach so closely that localized flow is set up between them [39, 40]. The level that the stress needs to attain to give lateral growth need not be very high, as shown by Figure 9, where voids are growing close to the notch root surface, or by the fact that voids can grow sideways in only gently necked tensile specimens.

The classical picture of fibrous crack growth is shown in Figure 10. Here a void forms around a second phase particle ahead of the growing crack (when sufficient shear strain, if necessary, has been developed at the particle) and the void grows in the hydrostatic tensile stress field. An internal neck is formed between the void and the crack tip and final separation occurs along a knife edge in three dimensions, to give a fracture surface composed of cusps and dimples, centred on the second-phase particles. The importance of nucleation strain is demonstrated in Figure 11, which shows that voids have formed around sulphide inclusions which are quite remote from the crack tip, but not around carbides which are close to the tip. A two-dimensional plane strain model of the necking process has been developed by Rice and Johnson [41], assuming a pre-crack which has straight sides and whose tip is situated at one inclusion spacing, X_o, from the nearest particle, of radius R_o. The crack tip opening at the point at which coalescence of the blunting crack and the expanding void first occurs is the initiation C.O.D., δ_i. Figure 12 then shows the predicted variation of δ_i/X_o with X_o/R_o. The Rice and Johnson model is also consis-

tent with the *stretch-zone-width* being the length of new surface along the blunted crack tip, up to the "knife-edge" separation point [42].

Experimental points for model metallurgical systems, which correspond to the initial assumptions, are shown in the same figure and agreement is obviously quite close. These points are for steels of fairly high hardening capacity and the specimens have been cut in the transverse orientation to give inclusions which are long in the thickness direction and have nearly circular cross-sections (for details, see [43, 44]). The agreement is nowhere near so good when a wider variety of steels and configurations is examined, Figure 13. Here, two main features are evident. On the one hand, specimens cut in the longitudinal orientation, where inclusions are elongated normal to the line of crack advance, show high values of δ_i. The increase occurs because it is necessary to spread high strains longitudinally as far as the ends of the inclusion. On the other hand, a number of structural steels, either as rolled plate or as castings, show values of δ_i lower then that predicted by the model, which assumed continuing hardening capacity.

The reason for this is that many steels lose their capacity for continued work hardening at high strains and flow begins to localize, eventually producing shear fracture along localized flow bands. If hardening capacity is exhausted at a stage where the void has begun to expand and the crack tip has blunted significantly, the flow localizes in the same manner as it would ahead of a semi-circular notch in a rigid/plastic material. Decohesion occurs along the slip-lines, which have the form of logarithmic spirals. Figure 14 shows the situation ahead of a crack tip in HY 80 [45] and Figures 15 to 17 show analogous decohesion ahead of machined notches of circular root radii in a 3Cr/Mo alloy steel, in a peak-aged Al4½Zn2½Mg alloy and in a 15% prestrained mild steel. In each case, hardening capacity has been exhausted and the material behaves as if it were plastic/rigid, with a specific fracture (shear) strain. A similar conclusion has been reached by Spretnak [46] who has related the critical shear strain to torsional fracture strains.

As yield strength increases, hardening capacity tends to decrease, and many high strength materials have toughnesses limited by this shear decohesion, rather than by void growth. The reasons for shear decohesion are not clear and need further investigation, but what is likely to happen in tempered alloy steel is that dislocations in the localized shear band tangle around carbide particles until such a density is reached that the interfaces decohere and resistance to flow decreases catastrophically. The whole band then "unzips" and fractures [45]. One experiment to test the effect would be to examine the shear fracture process in steels containing different volume fractions of carbide particles, but similar non-metallic inclusion contents. It may also be possible to lower interface cohesion by segregation of impurity elements.

The Rice and Johnson model [41] predicts that the minimum value of δ_i/X_o is approximately equal to 0.5, because this corresponds to the C.O.D. at which a logarithmic spiral slip-line from the semi-circular root of a blunted crack first "envelops" the expanding void. However, values lower than this can be obtained, because, in a material with very low hardening capacity, crack tip blunting is insignificant. Imagine a sharp crack in an array of holes, representing the voids formed at almost zero strain around second-phase particles, Figure 18 and [45]. The slip bands become localized in the directions of the nearest holes ahead of the crack tip and it is possible for decohesion to occur by shear along these bands before the crack tip

has blunted appreciably. The final fracture is crack-like and zig-zags from inclusion to inclusion, Figure 19. In a wrought steel, containing equiaxed inclusions, the sense of the zig-zag is random in any given cross section [45], but in cast weld metal [47] large "waves" or "ridges" are seen, on a macroscopic scale, on the fracture surface. Similar observations have been made on marageing steel [48].

The materials' factors that affect crack-tip ductility in the fibrous fracture process are therefore, primarily, the gross non-metallic or intermetallic inclusion content and the hardening capacity. To some extent, a change from plane strain to plane stress has a similar effect to that of increasing the hardening capacity, because the strain is spread over a wider area ahead of the crack tip and a higher C.O.D. is required to concentrate a given amount of strain in the region between the crack tip and the expanding void [49].

In materials which are clean from the point of view of gross inclusion content, the fracture strain, and hence δ_i, is governed by the extent to which localization occurs, although the fracture in commercial materials will be tempered carbides or fine scale (approximately 0.2μm diameter) intermetallics in aluminum alloys [50]. A good example of a low strain localized shear fracture in as-quenched 7075 Al-Zn-Mg alloy has recently been shown by Embury et al [51]; another disturbing possibility is that the accumulation of point defects in irradiated materials might give localization and lower the ductile fracture resistance of, for example, pressure-vessel steels [52].

The effect of hardening capacity is implicit in some of the finite element analyses, e.g., [41], but is brought out explicitly in a simple model due to Hahn and Rosenfield [53]. This rests on the experimental observation that the width of a plastic zone is proportional to n^2, where n is the work-hardening exponent. Development of the model then gives:

$$K_{IC} \propto \varepsilon_c^* \, n \sqrt{\sigma_Y} \qquad (11)$$

or

$$\delta_i \propto \varepsilon_c^* \, n^2 \qquad (12)$$

where ε_c^* is a critical fracture strain, dependent on the volume fraction of void nucleating particles. These forms are found to give quite good agreement with measured values of K_{IC} and δ_i in a range of commercial and pure aluminum alloys [50].

These models help to explain the C.O.D. required to initiate a ductile fracture at a crack tip, and the appropriate value of δ_i may be converted to an equivalent value of "K_i", using equation (3), assuming that all the fracture processes and associated plasticity are embedded in an enclave which is small compared with the dimensions of the cracked body. There is, however, no guarantee that this value of K_i is representative of instability in the body: there are situations, in marageing steels and high strength aluminum alloys, where it seems to be; there are others, in structural steels, where stable crack growth, under increasing K, may precede instability. It is not clear whether the unstable initiation can be associated with a process of shear band decohesion, or, as a corollary, whether the void growth mechanism can go unstable only by changing to the cleavage mode. The problems are compounded by the difficulties of calculating the

energy release rates for growing cracks containing plastic zones at their tips. It is of interest, however, to note that a value of δ_i = 0.175 mm, measured by Green [24] in A533B steel at 20°C, gives, using equation (3) a value of "K_i" equal to 180 MPam$^{1/2}$. This is of the same order as, although some 10-20% less than, the accepted value for K_{IC} at this test temperature.

Intergranular Fibrous Fracture

It is possible for fracture to progress by the linking of voids formed around second-phase particles, but to assume an intergranular fracture path. The conditions under which such behaviour occurs are relatively rare in low temperature tests, because it is necessary to find situations in which the intergranular fibrous fracture path is easier than a transgranular path. Generally, this is achieved if the density of weakly-bonded particles within the grains is low, but that on the boundaries is high.

One situation in which this occurs is the so-called *overheating* of *low sulphur* steels. At high austenitising temperatures, the majority of the sulphur in a low-sulphur steel can be taken into solution, removing most of the sulphide particles from within the grains. Then, if cooled at a critical rate [54], a fine sulphide distribution precipitates preferentially at the austenite grain boundaries to provide a low-energy fibrous path, Figure 20.

A similar effect can occur in *pure*, overaged, aluminum alloys [50]. Here, relatively finely-spaced, incoherent precipitates are formed on grain boundaries and are separated from the age-hardened grain by a soft precipitate free zone (PFZ). To a first approximation, it may be regarded that all the plastic deformation is confined to the soft PFZ region, so that intergranular fibrous fracture automatically ensues, but PFZs, albeit smaller, are present also in underaged alloys which fail in a transgranular manner. The situation here is, however, altered by the fact that, in the underaged alloys, intense slip bands can form and produce shear decohesion. If a comparison with commercial overaged alloys is made, the latter do not show fibrous intergranular facets, because it is quite easy to nucleate voids on the large second-phase particles which are present within the grain.

Generally, then, the occurrence of intergranular fibrous facets in low temperature fracture implies a toughness lower than that which would be obtained if no second-phase particles were present, but the toughness will be greater than that of a dirty material which shows a profusion of transgranular dimples.

Intergranular fibrous fractures are, of course, quite common features in high-temperature creep fracture. The voids are, again, generally held to be associated with second-phase-particles, and their nucleation is attributed to grain-boundary sliding, with subsequent growth under the action of the applied tensile stress. As for transgranular fibrous fracture, the nucleation criterion is one of a critical amount of shear strain, required to decohere the particle/matrix interface. In creep-resistant ferritic steels, it is usually assumed that the grain-boundary particles of importance are coarsely-tempered alloy carbides, although, in some cases, particles specifically added for grain-refinement, such as aluminum nitride, will also be of significance. There is evidence of a PFZ around the grain boundary in the quenched and tempered condition, which tends to enhance grain-boundary sliding compared with matrix deformation.

There are two interesting points concerned with the nucleation stage: th
first, related to the ease of nucleating cavities around particles, the
second, related to effects of stress-state. Consider a ferritic steel.
"Normal" resistance to nucleation is provided by the strength of the carbi
matrix interfacial bond. If this were weakened by segregation of minor
impurity elements, such as those which induce intergranular embrittlement
at low temperatures, the nucleation resistance would drop. An effect whi
could be explained in this way has been observed by Tipler et al [71] who
show that creep lives of (dirty) commercial ferritic steels are much
inferior to those of alloys of identical composition, with respect to the
major additions, but made from super-pure base material. An even more
deleterious effect on creep fracture might be obtained, if the boundary
contained particles, such as non-metallic inclusions, which possessed
almost no bonding with the matrix, because then the necessity for a nucle
tion stage could be removed. This situation could occur in an overheated
steel, as described above and, in a more practical sense, it might be per
tinent to note that the overheating heat treatment is not markedly differ
ent from that likely to be experienced by, for example, the coarse-grained
heat-affected zone of welded, thick-section boiler tube. It would be of
interest specifically to study creep void nucleation in overheated and no
overheated steels, but, more generally, to observe closely the types of
particles on which voids form in commercial steels, to distinguish effect
of trace elements on carbide cohesion from those of non-metallic inclusio

The nucleation process depends on shear strain, and therefore on the devi
toric component of any triaxial stress state. If creep fracture were si
nucleation-controlled, notch-strengthening would be expected to be observed
in all cases, because a higher applied stress would be necessary to achie
the critical shear strain in the constrained region around the notch. So
alloys do, indeed, exhibit notch-strengthening, but others, particularly
the higher strength alloys, fracture at lower stresses in notched bars th
in smooth specimens. Here, it may be deduced that the critical stage in
the creep fracture process is void growth, under the influence of the hi
tensile stress that exists in the constrained region. As for transgranul
cleavage fracture, it would be expected that the voids would start to gro
most rapidly some distance below the notch, but the situation may be con
fused if more nuclei are formed, as a function of time, by the higher cre
strains closer to the notch surface.

The mechanism of void growth is a function of stress and temperature.
Referring to Ashby's "deformation map" representation of behaviour [72]
it may be seen that (thermally-activated) slip is likely to dominate at
low temperatures and high stress levels, whereas diffusional growth assu
importance at higher temperatures and lower stresses. The former case ma
presumably be modelled by conventional low-temperature void coalescence
mechanisms, although for the assumed case of voids on a boundary surround
by a fairly narrow PFZ, it must be realized that, not only is the tensile
stress raised approximately to that of the matrix by constraint (as in a
soldered joint), but that this same constraint sets up high lateral
stresses, so that the voids are encouraged to grow rapidly in lateral
directions, as well as in the direction of the applied tensile stress
giving, presumably, rather shallow dimples. The diffusional growth model
has recently been treated in detail [73]; in simple terms, the stress
can do work if the specimen extends, and this provides a driving force fo
the diffusive flux of vacancies. The shape of the growing void depends,
inter alia, on the surface energy of the void surface, and the grain boun
dary energy. It has been suggested [71] that segregation of trace impurit
elements to grain boundaries might be able to modify this energy balance i

a manner such that growth rates were increased. At high growth rates, the periphery of the void becomes unstable with respect to random fluctuations and rapid, finger-like growth is observed [74]. Void growth may become so rapid in the lateral directions that individual intergranular facets present the appearance of intergranular cleavage fractures: arrest commonly occurs at triple points, however, and the final fracture of a specimen may be in certain circumstances related to a Griffith-type criterion for an arrested microcrack [75]. This behaviour would again be expected to give notch weakening.

There is not clear agreement on the relative importance of these various mechanisms with respect to the creep fracture of engineering alloys, mainly because the various possibilities have not been tested unambiguously. By analogy with low temperature fracture, points which need to be established are:

(1) the relative importance of nucleation and growth of voids; here, varying the type of nucleating particle and altering the stress state by means of notches should provide valuable information;

(2) the relative importance of different growth mechanisms has been placed on diffusional growth, because other growth mechanisms have been held to be of importance only in the very final stages of fracture, when the creep life is almost fully expended. This conclusion might, however, require re-examination if the nucleation stage dominated effects in pure research alloys, but not in commercial alloys containing non-metallic inclusions or large, incoherent, grain-refining particles at the boundaries. Furthermore, it may be possible to treat the lateral growth of voids in the highly constrained grain boundary region in terms of low-temperature void growth theory, with the time-dependence of the applied strain related to the thermally-activated glide stress. The various possibilities are presented neatly in the deformation maps [72]: it is primarily a question of testing rigorously which region on the map pertains to which particular commercial alloy, under a given set of conditions.

Clearly, the same general principles apply to a range of creep-resisting alloys: the example of ferritic steel has been used simply to indicate the large number of metallurgical variables which may have to be considered, before creep fracture can be explained properly.

FATIGUE-CRACK PROPAGATION AND MONOTONIC FRACTURE

A material's fracture toughness is a parameter of value, because it provides the engineer with a means of designing a structure to prevent the catastrophic propagation of any defect by fast fracture. If the structure is subjected to fluctuating stresses or to a corrosive environment, however, it is possible for "sub-critical" crack growth to occur, by fatigue or by stress-corrosion mechanisms. Under such circumstances, it is necessary to have a knowledge of crack growth rates under service stresses, so that regular inspection periods can be specified, without any danger of critical conditions for catastrophic failure having been attained in the interim. Fatigue crack propagation rates are primarily a function of the *range* of the applied stress, as expressed by the empirical law due to Paris [55]

$$\frac{da}{dN} = C \, \Delta K^m \qquad (13)$$

where da/dN is the increment in crack length per cycle, ΔK is the alter-

nating stress intensity: $\Delta K = K_{max}-K_{min}$, where K_{max} and K_{min} are the maximum and minimum values during the cycle; and C and m are constants. Equation (13) implies that, if log(da/dN) is plotted vs. log (ΔK), a straight line of slope m should be obtained. Early data seemed to fit this form, with values of m ≃ 4, although some values as high as m ≃ 10 were recorded.

More detailed measurements, over wider da/dN ranges, have shown that the log-log plot is not simply linear, but possesses three distinct regions. At low values of ΔK, there is a threshold, below which no crack growth can be detected; hence, da/dN = 0, log (da/dN) = $-\infty$. This is followed, at higher ΔK levels, by a linear region, where m values in the range 2-4 are found. The transition from the first region to the second region may show some curvature: here, the absolute growth rate, da/dN, values are low, but the 'm' values are high, probably because only a portion of the crack front advances on each cycle. Finally, at very high ΔK values, such that K_{max} approaches K_{IC}, high growth rates are obtained, together with high values of the exponent, m. These various effects have led to modifications of equation (13), one example of which is that due to McEvily [56], written as

$$\frac{da}{dN} = \frac{4\ A}{\pi\sigma_Y E}\ (\Delta K^2-\Delta K_{th}^2)\left\{1 + \frac{\Delta K}{K_c-K_{max}}\right\} \qquad (14)$$

where ΔK_{th} is the threshold value of ΔK, and A is a constant.

It should be emphasized that such expressions are empirical in nature and that a scientifically-based relationship must take account of the local fracture processes. The generally-accepted model of the basic fatigue-crack growth is that the crack tip opens and closes by reversed plastic flow each cycle. The reversed crack-tip opening in plane strain is then given, from a development of equation (3), by

$$\Delta\delta \simeq \frac{1}{2} \cdot \frac{\Delta K^2}{(2\sigma_c)\cdot E} \qquad (15)$$

where σ_c is the flow stress of the cyclically-hardened material. The amount of crack advance per cycle is taken as a fraction of $\Delta\delta$, representing the proportional lack of re-welding, and da/dN would then be predicted to be proportional to ΔK^2; i.e., m = 2. However, the crack may not propagate uniformly at every point along its thickness. In some places, grains will be more favourably oriented for slip, or second-phase particles may provide local stress concentrations. At low ΔK values, just above the threshold, only isolated patches of the crack front may grow at any one time. Suppose that, at a low ΔK value, ΔK_1, only 10%, say, of the crack front is growing. This gives a very low, *average*, overall rate. Locally, the region that is growing follows $da/dN \simeq C.\Delta K^2$. Now, at a higher ΔK value, ΔK_2, suppose that not only is the growing region propagating more quickly, because ΔK_2 is greater than ΔK_1, but also that more of the front is able to grow, because the higher local stresses implied by ΔK_2 are sufficient to produce flow in grains which were inactive at ΔK_1. The *average rate* at ΔK_2 will then lie above that extrapolated from ΔK_1, so that a value of m > 2 will be obtained.

This effect is not confined to the threshold region. Pickard et al [57] have shown that, in 316 stainless steel, there are discrepancies between the microscopic growth rate, measured from striation spacings on individual

facets, and the average rate, measured by the potential drop technique.. Only at $\Delta K \simeq 50$ MPa$\cdot$m$^{1/2}$, did the rates coincide. In the range ΔK = [illegible] MPa$\cdot$m$^{1/2}$ to $\Delta K = 50$ MPa$\cdot$m$^{1/2}$, however, the rate was linear, with m = 4.2. It is clear that the basic plane strain continuum model, which predicts m = 2, needs to be modified at the lower ΔK levels (which actually constitute the majority of the lifetime in most structures), to take account of the non-uniformity of crack growth. Work on materials of different amounts of anisotropy and different cyclic hardening characteristics would help to elucidate these processes.

Behaviour at high K_{max} values depends on the monotonic fracture mechanisms that lead to catastrophic failure at K_{IC}. Ritchie and Knott [58, 59] have examined the situation with regard to transgranular and intergranular cleavage in mild steel and in temper embrittled low alloy steel. In both cases, the sequence of events is similar. At relatively low K_{max} values, isolated cleavage facets are visible on the fracture surface, intermixed with fatigue striations. As K_{max} increases, the proportion of facets increases, and they occure more as "bursts", giving rise to discontinuities in the graph of a vs. N, and to consequent increases in da/dN, which tend to give high apparent values of m. Ritchie and Knott were able to rationalise effect of R-ratio (K_{min}/K_{max}) on growth rate and to relate the onset of the cleavage burst in coarse-grained mild steel to the attainment of a local stress similar to the value, σ_f, required to give cleavage fracture in notched-bar tests.

It is evident that the proportion of cleavage facets increases in a smooth fashion with K_{max} [60], but the reasons for this have not been fully investigated. Cyclic hardening increases the flow stress and can hence produce local tensile stresses which are greater than those at similar K levels in pre-cracked, but normalized, specimens: on the other hand, the cyclic strain presumably increases σ_f, in the same manner as does monotonic pre-strain [25]. Additionally, the cyclic frequency is likely to affect the ease of propagating a single microcrack into adjacent grains. The processes would be well studied in steels possessing not only different grain sizes, but also different degrees of texture, or grain orientation.

In ductile steels and non-ferrous alloys, the termination of fatigue crack growth is a fibrous rupture, which may, or may not, occur at a K_{max} value equal to K_{IC}. Differences may occur because, in the K_{IC} test, the final fatigue pre-crack must be grown at a K_{max} value $\leq 0.67\ K_{IC}$, so that effects of cyclic hardening or strain localization are likely to be less significant than in the fatigue test, where the crack grows through progressively hardened material.

Generally, it should be realized that void expansion will begin at K_{max} values substantially less than K_{IC}, so that high growth rates will be characterized by an increasing proportion of fibrous fracture compared with fatigue. It should be possible to quantify the average void diameter at a given K level using results from fibrous fracture models [41] and so calculate the area and hence the amount, of crack growth due to dimples. It has recently been shown that the K_{max} values which characterize the termination of fatigue crack growth in several cast steels corresponds to C.O.D. values, calculated from equation (15), which are approximately equal to the spacings of void-forming particles [61].

Generally, monotonic fracture modes in fatigue assume more significance at high $\Delta K(K_{max})$ levels. In terms of lifetime, this is very close to final fracture, because the cracks are growing rapidly. Such fractures have,

however, helped to explain effects of R-ratio, anomalously high m values, and other causes of "scatter" [59]. Probably the most important effect is that of intergranular fracture, due to embrittlement. Fibrous fractures are usually associated with K_{max} values very close to K_{IC}, but serious deterioration of fatigue behaviour can occur if the volume fraction of particles is very high or if the particles are closely spaced. Significant effects have been observed in overheated steels [54], where sulphides are closely spaced on prior austenite grain boundaries; in aluminum alloys, [62] where voids form around fine scale intermetallics; and in 316 stainless steel weld metal, [57] which contains a high volume fraction of deoidation products. Examples of void growth here are shown in Figures 21 and 22.

A final point concerns the presence of apparent "cleavage" fracture during fatigue in pure aluminum alloys [63]. As shown in Figure 23 cleavage-like facets may be seen in pure Al-Cu alloys and detailed examination shows that they are macroscopically on {100} planes. However, the process is not catastrophic, and there is no increase in growth rate with R-ratio. The facets are, in fact, covered with very fine striations and have the appearance that they do because the crack-tip opening and closing is achieved by movement of dislocations on well-defined, intersecting {111} slip planes. A similar effect has been seen at low ΔK values in 316 stainless steel [57] and in aluminum bronze [64]. At higher ΔK values, the appearance is lost, because the plastic zone is no longer confined to single grains.

CONCLUSIONS

Of the various micromechanisms of fracture, understanding has progressed most deeply with respect to transgranular cleavage. Future research will be directed towards the adoption of a full statistical approach to the fracture of spheroidite microstructures and the categorization of the change from carbide/matrix propagation to packet/packet propagation in highly dislocated lath microstructures. The value of σ_f leads, on the one hand, to calculations of γ_p, whose magnitude still needs detailed explanation, and, on the other, to K_{IC} values. The same principles may be applied to intergranular fractures, although interpretations of γ_p and "critical distance" will here require very careful consideration. Transgranular fibrous fracture in a matrix of high hardening capacity is readily related to void growth mechanisms, but, in many commercial materials, the ductility is ultimately limited by fast shear fracture. Exhaustion of hardening capacity, by prestrain, or by cyclic hardening, is therefore of extreme significance to a material's crack tip ductility.

Hopefully, the paper has shown that much insight into the meaning of toughness parameters may be gained by study of the local micro-mechanisms of fracture. Such studies not only provide confidence in the use of toughness measurements for the quantitative engineering design of large structures to resist fast fracture: they serve also to identify the microscopic features which lead to the easy formation of cracks or voids, and so make possible a quantitative metallurgical design of micro-structures which will be particularly resistant to fast fracture.

ACKNOWLEDGEMENTS

The author wishes to thank Professor R. W. K. Honeycombe for provision of research facilities, and Mr. J. Q. Clayton, Mr. D. A. Curry, Mr. A. C. Pickard and Dr. R. F. Smith for useful discussions. The help of Mr. B. Barber, Mrs. C. E. Bishop and Mr. S. Charter in preparing the paper is gratefully acknowledged.

REFERENCES

1. KNOTT, J. F., "Fundamentals of Fracture Mechanics", Butterworths, London, 1973.
2. TRACEY, D. M., Ph. D. Thesis, Brown University, 1973 and RICE, J. R., Third International Congress on Fracture, Munich, 1973, paper I-441.
3. LARSSON, S. G. and CARLSSON, A. J., J. Mech. Phys. Solids, 21, 1973, 263.
4. LOW, J. R., Symposium on Relation of Properties to Microstructure, ASM, 1954, 163.
5. PETCH, N. J., "Fracture 1959", edited by B. L. Averbach et al, John Wiley/Chapman and Hall, 1959, 54.
6. COTTRELL, A. H., ibid, 20.
7. SMITH, E., Proceedings of the Conference on "The Physical Basis of Yield and Fracture", Inst. of Physics and Phys. Soc., 1966, 36.
8. LINDLEY, T. C., OATES, G. and RICHARDS, C. E., Acta Met., 18, 1973, 1127.
9. COTTRELL, A. H., Symposium on "The Relation Between the Structure and Mechanical Properties of Metals", National Physical Laboratory, HMSO, (London), 1963, 456.
10. KNOTT, J. F., J. Iron and Steel Inst., 204, 1966, 104.
11. WILSHAW, T. R., RAU, C. A. and TETELMAN, A. S., Eng. Frac. Mech., 1, 1968, 191.
12. GRIFFITHS, J. R. and OWEN, D. R. J., J. Mech. Phys. Solids, 19, 1971, 419.
13. OWEN, D. R. J., NAYAK, G. C., KFOURI, A. P. and GRIFFITHS, J. R., Int. J. Num. Meth. Engng., 6, 1973, 63.
14. COTTRELL, A. H., Trans. A.I.M.M.E., 212, 1958, 192.
15. McMAHON, C. J. and COHEN, M., Acta Met., 13, 1965, 591.
16. ALMOND, E. A., TIMBRES, D. H. and EMBURY, J. D., "Fracture 1969", edited by P. L. Pratt, Chapman and Hall, London, 254.
17. CURRY, D. A. and KNOTT, J. F., Metal Science, 10, 1976, 1.
18. FEARNEHOUGH, G. D., M. Sc. Thesis, University of Manchester, 1964.
19. KNOTT, J. F., "Mechanics and Physics of Fracture", Inst. of Physics and Metals Society, Cambridge, 1975, 86.
20. SAUNDERS, G. G., Ph. D. Thesis, Cambridge University, 1975.
21. DOLBY, R. E. and KNOTT, J. F., J. Iron and Steel Inst., 210, 1972, 857.
22. BROZZO, P., BUZZICHELLI, G., MASCANZONI, A. and MIRABILE, M., Report CSM 426V Centro Sperimentale Metallurgico, Rome, April, 1976.
23. NAYLOR, J., "Grain Boundaries", Jersey, 1976, Institution of Metallurgists, F.13.
24. GREEN, G., Ph. D. Thesis, Cambridge University, 1975.
25. GROOM, J. D. G. and KNOTT, J. F., Metal Science, 9, 1975, 390.
26. COTTRELL, A. H., Tewksbury Symposium on Fracture, University of Melbourne, 1963, 1.
27. KELLY, A., TYSON, W. R. and COTTRELL, A. H., Phil. Mag., 15, 1967, 567.
28. RICE, J. R. and THOMSON, R., Phil. Mag., 29, 1974, 73.
29. RITCHIE, R. O., KNOTT, J. F. and RICE, J. R., J. Mech. Phys. Solids, 21, 1973, 395.
30. SCHULZE, H. D., private communication.
31. PARKS, D. M., Conference on "Micromechanical Modelling of Flow and Fracture", Troy, 1975, ASME Paper No. 75-Mat-9, (to appear in J.E.M.T.).

32. McMAHON, C. J., "Mechanics and Physics of Fracture", Inst. Physics and Metals Society, Cambridge, 1975, 192.
33. TAIT, R. A. and KNOTT, J. F., "Fracture 1977", edited by D. M. R. Taplin, University of Waterloo Press, 1977, Vol. II.
34. KULA, E. B. and ANCTIL, A. A., J. of Materials, 4, 1969, 817.
35. RELLICK, J. R. and McMAHON, C. J., Met. Trans., 5, 1974, 2349.
36. McMAHON, J. A. and THOMAS, G., "Microstructure and Design of Alloys", Cambridge, 1973, Iron and Steel Inst./Inst. Metals, 1, 180.
37. RITCHIE, R. O., GENIETS, L. C. E. and KNOTT, J. F., ibid, 124.
38. McCLINTOCK, F. A., Int. J. Fracture Mechanics, 4, 1968, 101.
39. THOMASON, P. F., J. Inst. Metals, 96, 1968, 360.
40. BROWN, L. M. and EMBURY, J. D., "Microstructure and Design of Alloys", Cambridge 1973, Iron and Steel Inst./Inst. Metals, 1, 164.
41. RICE, J. R. and JOHNSON, M. A., "Inelastic Behaviour of Solids", edited by M. F. Kanninen et al, McGraw Hill, New York, 1970, 641, see also reference [2].
42. GREEN, G., SMITH, R. F. and KNOTT, J. F., "Mechanics and Mechanisms of Crack Growth", Cambridge, 1973, British Steel Corporation, 58.
43. SMITH, R. F. and KNOTT, J. F., "Practical Applications of Fracture Mechanics in Pressure-Vessel Technology", Inst. Mech. Engrs., 1971, 65.
44. GREEN, G. and KNOTT, J. F., "Micromechanical Modelling of Flow and Fracture", Troy, 1975, ASME paper 75-Mat-10, (to appear in J.E.M.T.).
45. CLAYTON, J. Q. and KNOTT, J. F., Metal Science, 10, 1976, 63.
46. GRIFFIS, C. A. and SPRETNAK, J. W., Trans. Iron and Steel Inst., Japan, 9, 1969, 372.
47. SAUNDERS, G. G. and KNOTT, J. F., The Welding Institute Research Bulletin, 16, 1975, 106.
48. BEACHEM, C. D. and YODER, G. R., Met. Trans., 4, 1973, 1145.
49. RITCHIE, R. O., SMITH, R. F. and KNOTT, J. F., Metal Science, 9, 1975, 485.
50. GARRETT, G. G. and KNOTT, J. F., Second Int. Conf. on Mechanical Behaviour of Materials, Boston, August, 1976.
51. EMBURY, J. D. et al, "Unstable Shear Fracture in a 7075 Aluminum Alloy" Acta Met., to be published.
52. WULLAERT, R., private communication.
53. HAHN, G. T. and ROSENFIELD, A. R., A.S.T.M., STP 432, 1968, 5.
54. RITCHIE, R. O. and KNOTT, J. F., Met. Trans., 5, 1974, 782.
55. PARIS, P. C., "Fatigue, An Interdisciplinary Approach", Sagamore, New York, 1964, 107.
56. McEVILY, A. T., "Microstructure and Design of Alloys", Cambridge, 1973, Iron and Steel Inst./Inst. of Metals, 2, 204.
57. PICKARD, A. C., RITCHIE, R. O. and KNOTT, J. F., Metals Technology, 2, 1975, 253.
58. RITCHIE, R. O. and KNOTT, J. F., Mat. Sci. and Engng., 14, 1974, 7.
59. RITCHIE, R. O. and KNOTT, J. F., Acta Met., 21, 1973, 639.
60. BEEVERS, C. J., COOKE, R. J., KNOTT, J. F. and RITCHIE, R. O., Metal Science, 9, 1975, 119.
61. EL SOUDANI, S. and KNOTT, J. F., SCRATA Product Technology Panel Report, to be published.
62. GARRETT, G. G. and KNOTT, J. F., Met. Trans., 6A, 1975, 1663.
63. GARRETT, G. G. and KNOTT, J. F., Acta Met., 23, 1975, 841.
64. PICKARD, A. C., RITCHIE, R. O. and KNOTT, J. F., Fourth Int. Conf. on The Strength of Metals and Alloys, Nancy, August-September, 1976.
65. KNOTT, J. F., J. Mech. Phys. Solids, 15, 1967, 97.
66. WILSHAW, T. R., J. Iron and Steel Inst., 204, 1966, 936.
67. OATES, G., J. Iron and Steel Inst., 207, 1969, 353.
68. LOW, J. R., "Iron and Its Dilute Solid Solutions", Wiley, New York, 1963, 255.
69. HOLZMANN, M. and MAN, J., J. Iron and Steel Inst., 209, 1971, 836.

70. CHIPPERFIELD, C. G. and KNOTT J. F., Metals Technology, 2, 1975, 45.
71. TIPLER, H. R., TAYLOR, L. H., and HOPKINS, B. E., Met. Sci., 4, 1970, 167.
72. ASHBY, M. F., "Fracture 1977", edited by D. M. R. Taplin, University of Waterloo Press, 1977, Vol. I.
73. RAJ, R. and ASHBY, M. F., Acta Met., 23, 1975, 653.
74. WINGROVE, A. L. and TAPLIN, D. M. R., J. Materials Sci., 4, 1969, 789.
75. FLECK, R. G., BEEVERS, C. J. and TAPLIN, D. M. R., Metal Sci., 2 1974, 226.
76. KOTILAINAN, H. and TÖRRÖNEN, K., "Fracture 1977", edited by D. M. R. Taplin, University of Waterloo Press, 1977, Vol. II.
77. KING, J. E., SMITH, R. F. and KNOTT, J. F., "Fracture 1977", edited by D. M. R. Taplin, University of Waterloo Press, 1977, Vol. II.

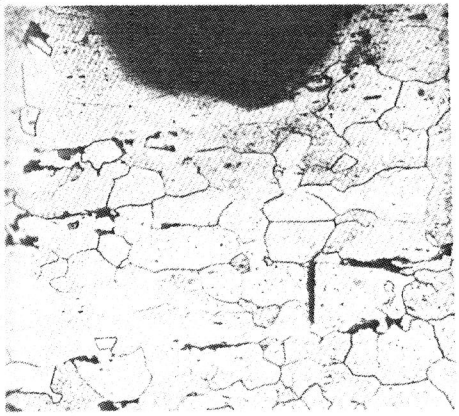

Figure 1 Formation of Cleavage Crack Below Notch in Mild Steel X 100

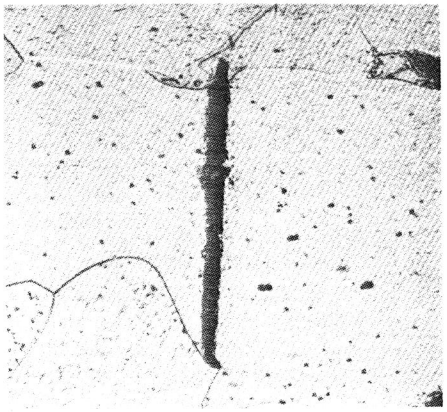

Figure 2 Detail of Crack in Figure 1. Note Non-Propagating Crack Nucleus in Carbide at Top of Micrograph. X 500

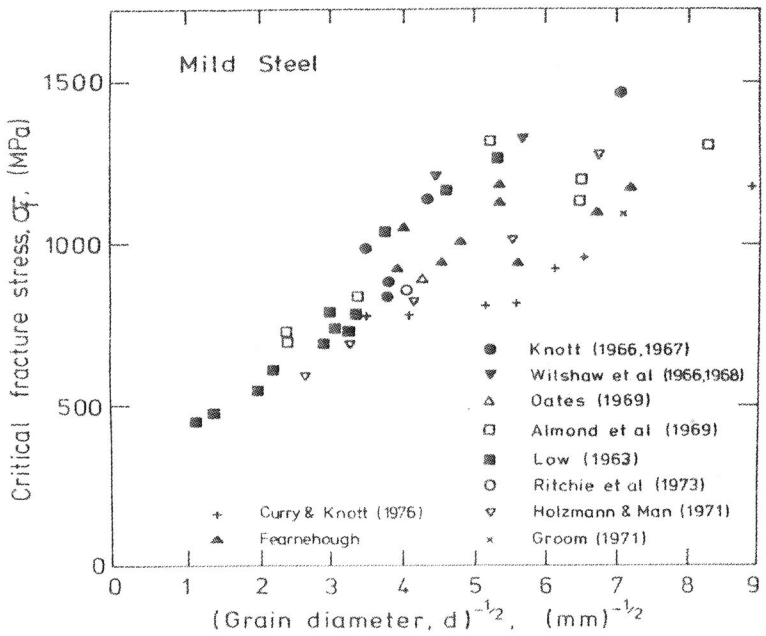

Figure 3 Experimental Vaues of Local Fracture Stress Plotted vs. The Reciprocal Square Root of Grain Size. Data for Mild Steel Taken from [17], [18], [10], [65], [66], [11], [67], [16], [68], [29], [69] and [25].

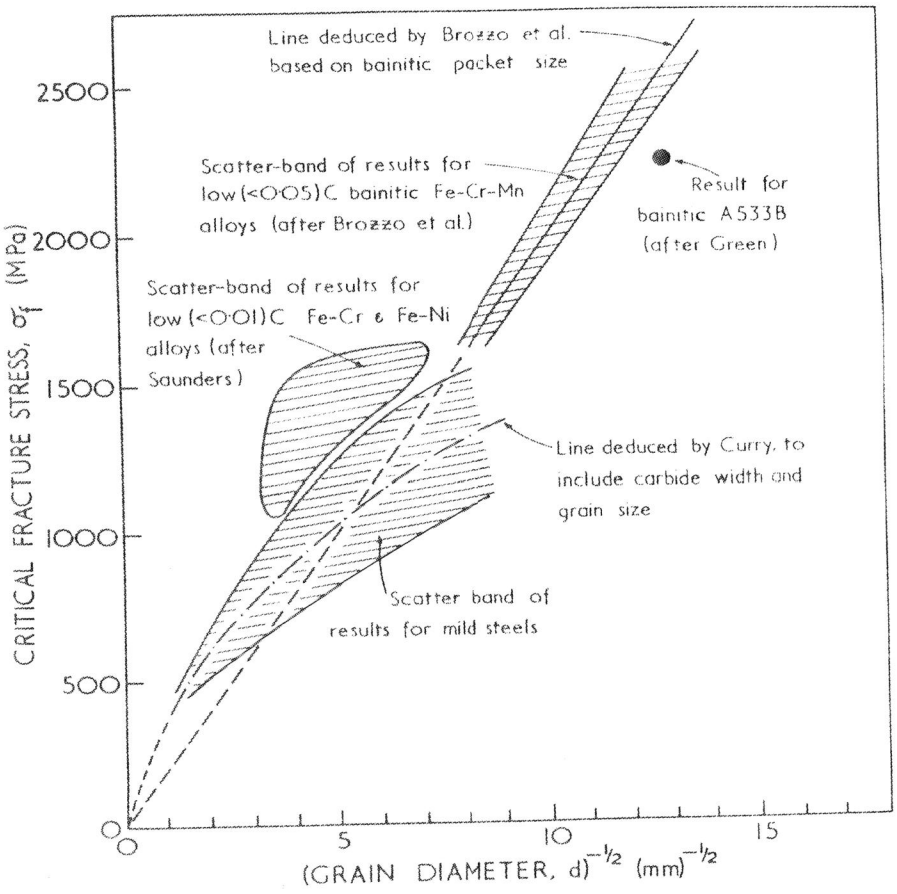

Figure 4 As Figure 3, but Extended to Cover Lath Bainites [22], A533B [24], and low C Fe-Ni and Fe-Cr Alloys [20].

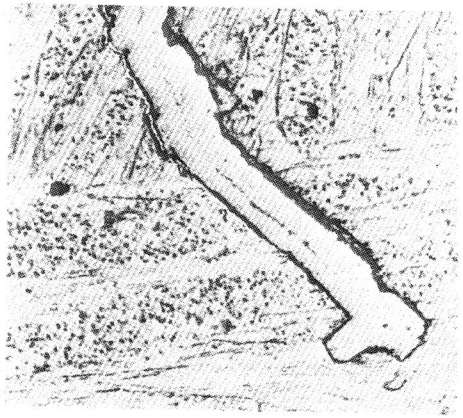

Figure 5 Microcrack in HY80 Auto-Tempered Martensite; After [21] X 7500

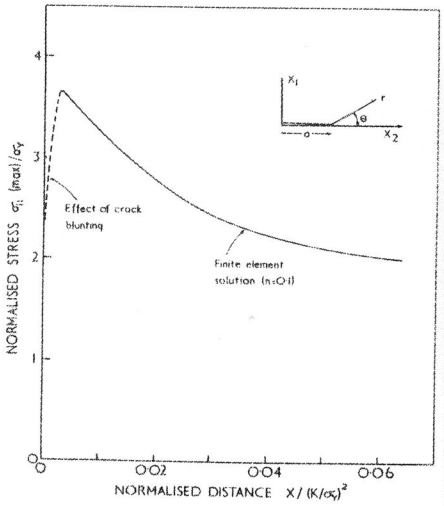

Figure 6 Stress Distribution Ahead of a Blunting Crack; After [2]

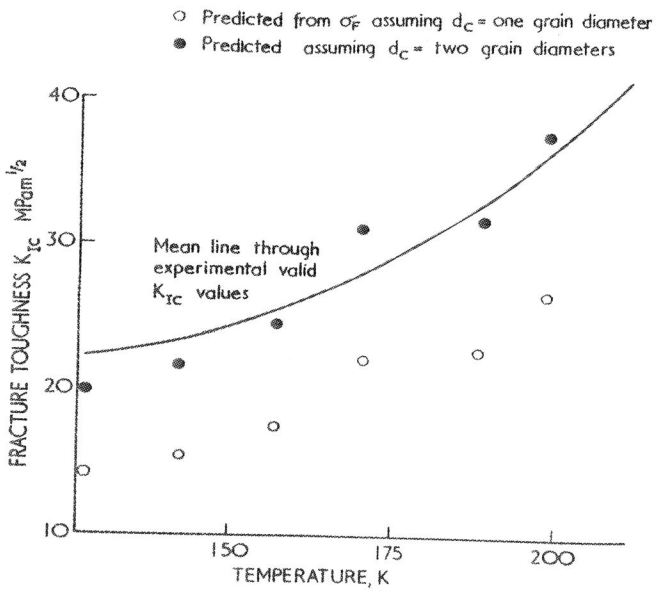

Figure 7 Comparison Between Experimental Values of K_{IC} and Those Predicted from σ_f; after [29]

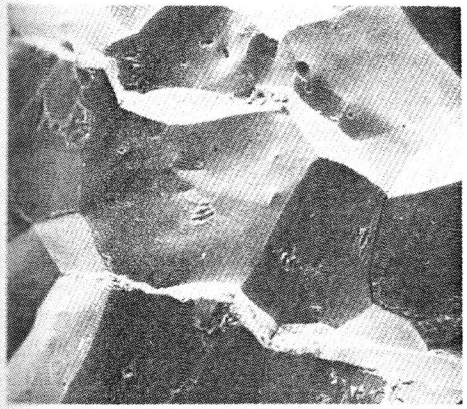

Figure 8 Fracture Surface of Embrittled As-Quenched Martensite in Low-Alloy Steel Containing Mn and P (courtesy J. Q. Clayton) X 170

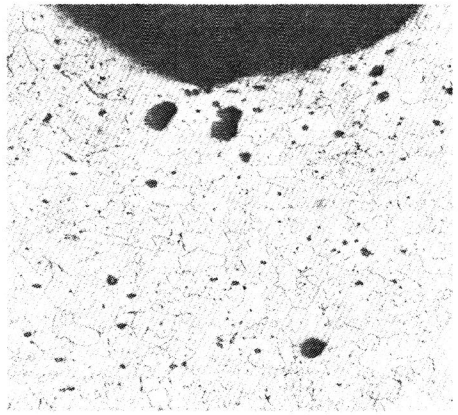

Figure 9 Void Expansion Near Notch Root Surface, Where Lateral Stress is not High X 70

Figure 10 Fibrous Crack Growth in Free-Cutting Mild Steel (courtesy R. F. Smith) X 600

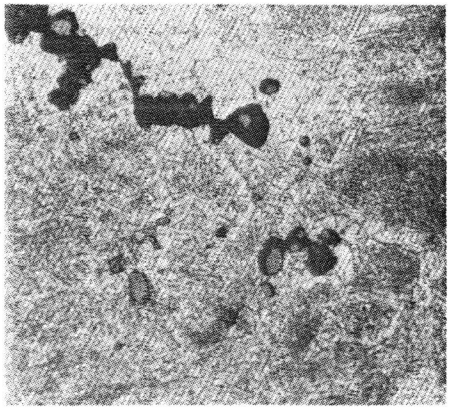

Figure 11 Fibrous Crack Growth in Free-Cutting, Spheroidized En8 (0.4C) (courtesy R. F. Smith) X 600

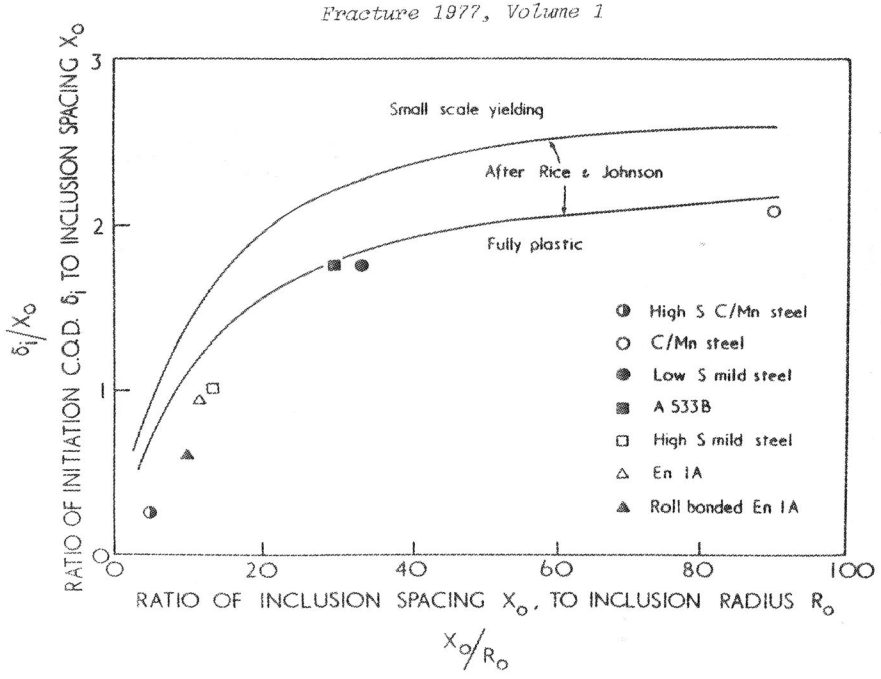

Figure 12 Predictions of Rice and Johnson Compared with Experimental Values of δ_i in Transverse Specimens; after [44]

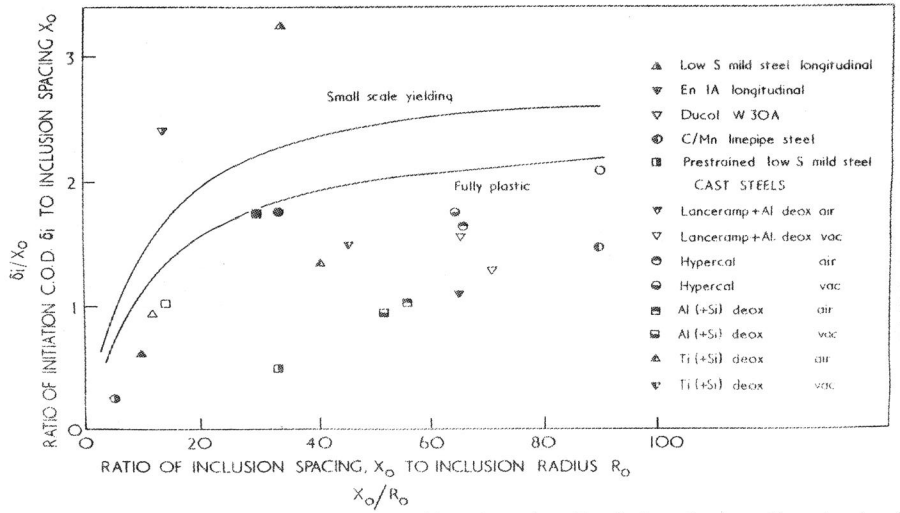

Figure 13 As Figure 12, but Including Longitudinal Specimens, Prestrained Specimens and Cast Steels. Data from [24], [42], [43], [44], [61], and [70]

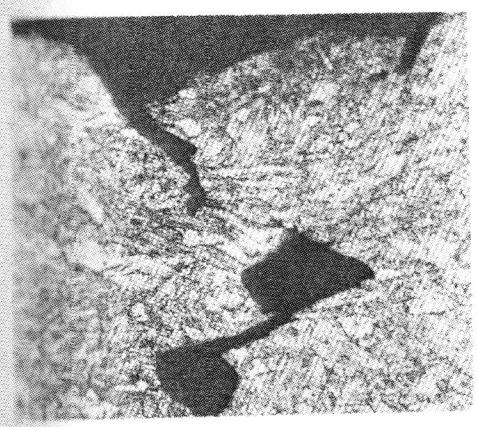

Figure 14 Details of Crack-Tip Linkage in HY80 (courtesy J. Q. Clayton) X 700

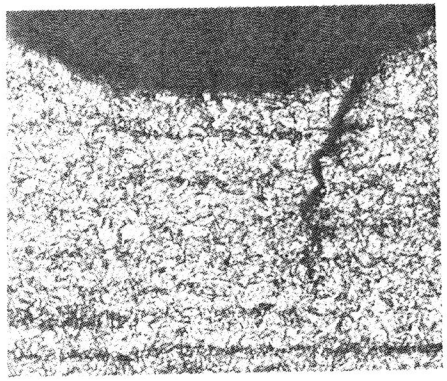

Figure 15 Shear Decohesion Along Slip Line in Cr Mo Alloy Steel; After [45] X 250

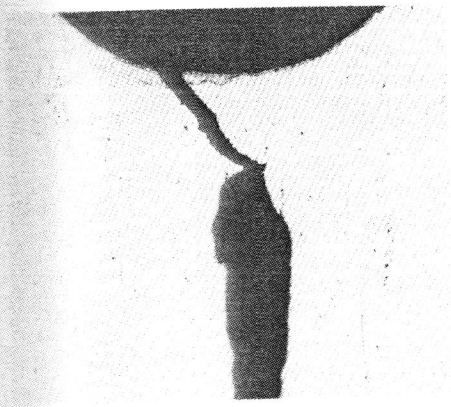

Figure 16 Shear Decohesion in Peak Aged Al-$4^{1/2}$ Zn-$2^{1/2}$Mg Alloy (courtesy R. F. Smith) X 35

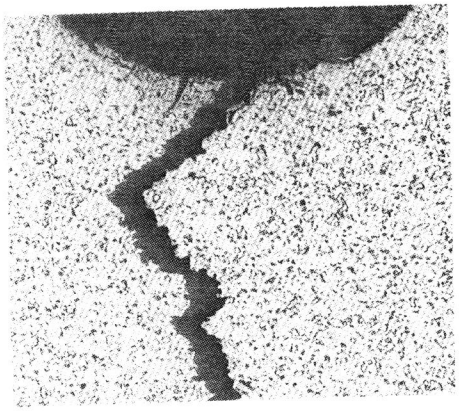

Figure 17 Shear Decohesion in En 1A Prestrained 15% (courtesy R. F. Smith) X 35

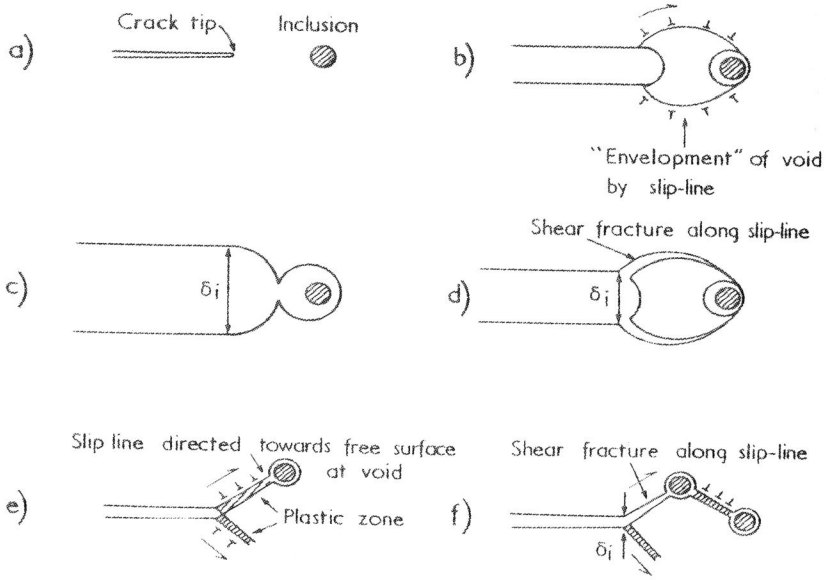

Figure 18 Modes of Fibrous Fracture; After [41] and [45].

a) Crack Tip and Inclusion
b) Envelopment of Void by Logarithmic Spiral Slip-Line
c) Void Coalescence by Internal Necking in Hardening Matrix
d) Development of b) to Give Shear Decohesion as in Figure 14
e) Direction of Shear Band Towards Void in Non-Hardening Material
f) Decohesion Along Shear Band

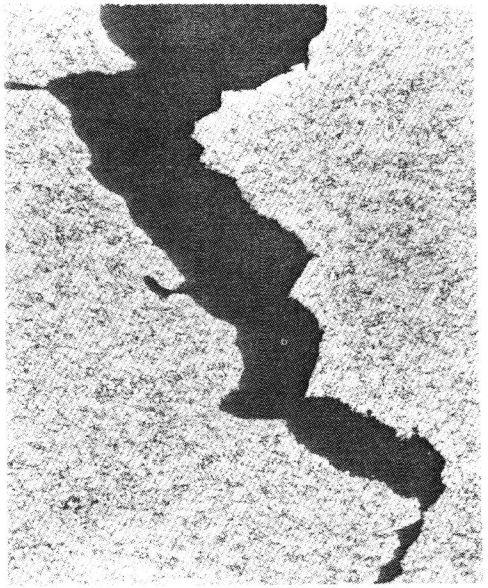

Figure 19 Zig-Zag Fracture in HY80, Prestrained 20%; After [45] X 150

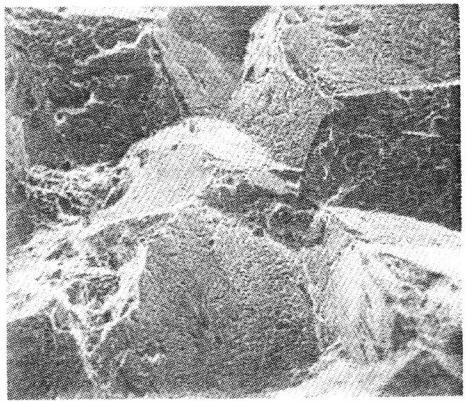

Figure 20 Fracture Surface in Overheated, As-Quenched Steel. Note Dimples on Intergranular Facets, and Contrast with Figure 8. (Courtesy J. Q. Clayton) X 170

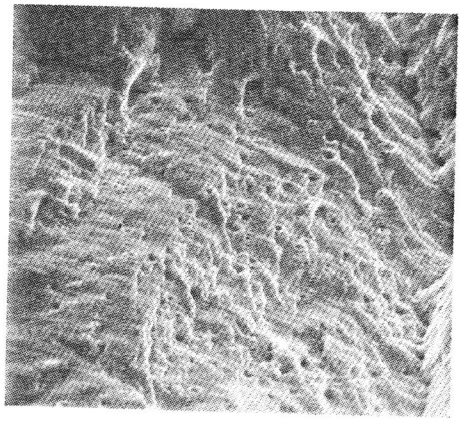

Figure 21 Striations and Voids in 316 Stainless Steel Weld Metal, ΔK = 24.6 MPa $m^{1/2}$, R = 0.5; After [57]

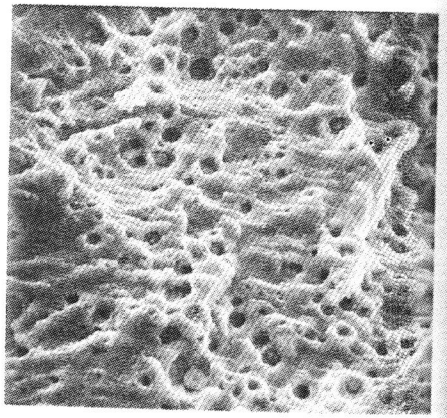

Figure 22 As Figure 21, but with ΔK = 33 MPa $m^{1/2}$, R = 0.3. (Cleaner) Plate Material Shows Striations, but no Voids, at These ΔK Levels; After [57]

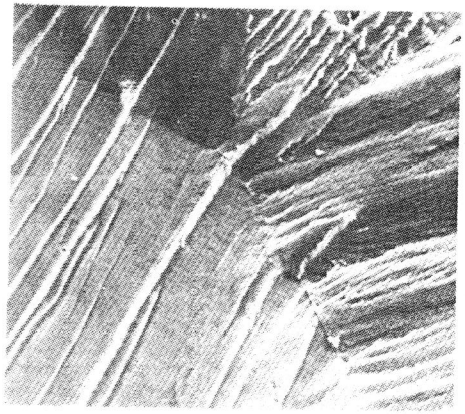

Figure 23 "Cleavage" facets in Coarse-Grained, Pure Al-Cu Alloy. Note Fine Striations on the Surface, which help to show that Process in one of Crystallographic Fatigue. A Macroscopic Opening in the [001] Direction can be achieved by Gliding on {111} Planes. In terms of Dislocations:

$$a[001]_{(001)} \rightarrow \frac{a}{2}[0\bar{1}1]_{(111)} + \frac{a}{2}[011]_{(\bar{1}\bar{1}1)} \quad ; \text{ After [63]}$$